Journal of Electromagnetic Waves and Applications, 2013
Vol. 27, No. 12, 1483–1495, http://dx.doi.org/10.1080/09205071.2013.816877

Taylor & Francis
Taylor & Francis Group

Design of concentric ring antenna array for a reconfigurable isoflux pattern

Alberto Reyna Maldonado[a]*, Marco A. Panduro[a], Carlos del Rio Bocio[b] and Aldo L. Mendez[a]

[a]*Unidad Académica Multidisciplinaria Reynosa-Rodhe, Universidad Autónoma de Tamaulipas (UAT), Carretera Reynosa-San Fernando, Reynosa, Tamaulipas 88779, México;* [b]*Universidad Pública de Navarra, Arrosadia Campus, UPNA, Pamplona, Spain*

(*Received 1 March 2013; accepted 14 June 2013*)

This report presents a novel design of concentric ring antenna array for a reconfigurable isoflux pattern. The array considers 61 disk patch antennas including mutual coupling by using the cavity model at the frequency of 2.8 GHz. The problem consists in finding out a few levels of excitations for the disk patch antennas. Harmony search algorithm and particle swarm optimization are implemented for this optimization problem. This novel design permits to reduce the complexity of the antenna hardware in the whole antenna system mounted in a satellite, where the volume occupation and heat dissipations are critical issues.

1. Introduction

Many modern communication applications require satellites to fly around the Earth at different altitudes with a global coverage for providing uniform power density.[1] This is usually referred to an isoflux pattern.[2] These satellites are called highly elliptical orbit (HEO) satellites.[3,4] In this case, these systems require an antenna system with a reconfigurable coverage pattern, i.e. these satellites require a capable antenna system to change the properties of the radiation. For instance, the antenna gain has to be different at the edge of coverage (EOC) for an orbit flight.[5] Furthermore, a non-complex antenna array is mandatory for avoiding more weight, volume, complex feeding systems, and complex heat dissipation systems.

This paper presents the design of concentric rings antenna arrays for a reconfigurable wide coverage pattern. Patch antenna arrays (PAA) are considered in this study, because they shape a singular beam pattern, low mass, and weight.[6] The purpose of this paper is to present a design of a PAA for a reconfigurable isoflux pattern, with fewer levels of excitations to diminish the hardware complexity. It is considered disk patches as antenna elements simulated by the cavity model.[7] The mutual coupling is regarded by the open-circuit voltage approach.[8] Then, the design process considers the optimization of the excitations of each patch antenna. In order to use fewer levels of excitations to diminish the hardware complexity, a concentric excitation is considered across the antenna array, i.e. uniform excitation in each ring, but a non-uniform excitation among rings. Since the complexity of the problem is very high, particle

*Corresponding author. Email: alberto.reynam@outlook.com

swarm optimization (PSO) [9] and harmony search algorithm (HSA) [10,11] are used as optimization approach. To the best of the author's knowledge, the design of concentric rings antenna arrays for a reconfigurable isoflux pattern has not been presented previously.

The remainder of the paper is organized as follows. Section 2 states the antenna array design problem we are dealing with. Section 3 describes the employed evolutionary optimization algorithms. Section 4 presents and discusses the simulation results. Finally, the summary and conclusions of this work are presented in Section 5.

2. Problem statement

Assume a concentric rings antenna array shown in Figure 1 of N_T disk patch antennas; the normalized radiation pattern is given by [12],

$$P(\theta,\varphi) = |g(\theta,\varphi)|\left|\left(I_c + \sum_{p=1}^{N_r}\sum_{m=1}^{N_p} I_{pm} e^{jk[r_p u\cos\varphi_m + r_p v\sin\varphi_m]}\right)\right| \tag{1}$$

where

$$g(\theta,\varphi) = E_\theta\widehat{\theta} + E_\varphi\widehat{\varphi} \tag{2}$$

$$V = IZ \tag{3}$$

Moreover, $u=\sin\theta\cos\varphi$, $v=\sin\theta\sin\varphi$, N_r represents the number of rings, N_p represents the number of elements on ring p, $\varphi_m = 2\pi\ (m-1)/N_p$ represents the angular position of the element m on the ring p, and r_p represents the radius of ring p. The k is the wave number. The h is the thickness of the dielectric. The I_c is the current excitation of the central element. The term I_{pm} is the current excitation of the element m on the ring p. These current excitations are defined in a vector $I=\{I_c, I_{11}, I_{12}, \ldots, I_{Nr\ Np}\}$. The vector V represents the voltage excitations. The elements of V are grouped into levels voltages. The center element and every antenna element of each ring are fed by a

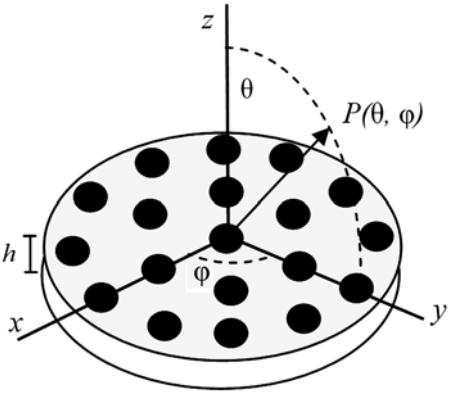

Figure 1. Patch Concentric Ring Antenna Array.

different level of voltage excitation defined as $L=\{l_1,l_2,\ldots,l_{Nr+2}\}$ where l_1 is the voltage coefficient value of the center element and l_{Nr+2} is the voltage coefficient for the elements of the bigger ring. Then, the antenna array is able to reconfigure their radiation properties by using the same antenna elements with the same spatial distribution but excited with different voltage excitations. The results in [13,14] showed that the spatial distribution of the rings is very suitable to be sparse increasingly to the maximum aperture for providing an isoflux shape. To achieve so, we propose to set the spacings among the rings as $S_p=\lambda/2+(\lambda/10)(p-1)$ since these spacings must be fixed a priori the optimization for the reconfigurable isoflux pattern. Where S_p is the spacing between the ring p and the ring $(p-1)$. Then, the first spacing is between the first ring and the central element, i.e. the radius of the first ring $(p=1)$ is $S_1=r_1$. Otherwise, the spacing among the antenna elements in the ring p is $q_p=2\pi r_p/N_p$. Equation 2 is the element pattern $g(\theta, \varphi)$ of a disk patch antenna. The terms E_θ and E_φ are the normalized pattern components at the fundamental mode TM_{11} of each disk patch antenna via the well-known cavity model,[7]

$$E_\theta = \cos\varphi J_1(ak_0\sin\theta) \tag{4}$$

$$E_\varphi = \cos\theta\sin\varphi J_1(ak_0\sin\theta) \tag{5}$$

where the a is the radius of the patch at the resonance frequency. The J_1 is the Bessel function of the first order. For the analysis of mutual coupling, it is obtained the impedance matrix Z based on the assumptions of the well-known equivalence theorem.[15] The centers of each pair of disk patch antennas are at a distance d within the antenna array, as shown in Figure 2.

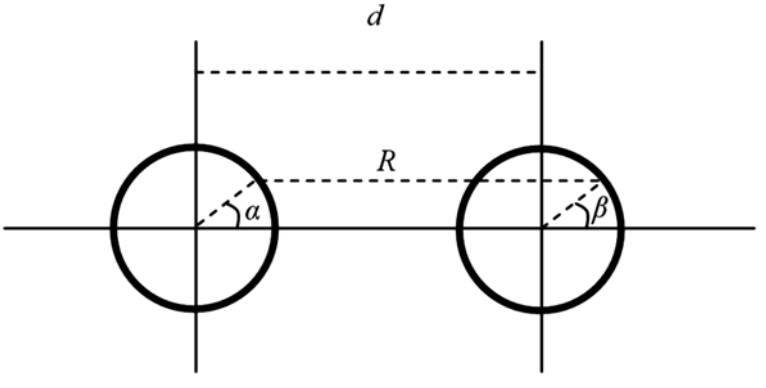

Figure 2. Pair of disk patches within the PAA.

Then, the self impedance z_{11} is obtained by the input resistance R_{in} and reactance X_{in} as follows [12,16]:

$$z_{11} = R_{in} + jX_{in} \tag{6}$$

And, the formulation of the mutual impedance z_{12} between any pair of disk patch antennas within the array is obtained as follows [17]:

$$z_{12} = -\frac{jf_r\varepsilon_0}{2}aE_0J_1(ka)\int_{\beta=0}^{2\pi}\int_{\alpha=0}^{2\pi}\cos(\alpha)\cos(\beta)\cos(\alpha-\beta)\frac{e^{-jkR}}{R}d\alpha d\beta \tag{7}$$

where the term E_0 is the modal coefficient for the mode TM_{11}. The R represents the distance between the source of the first patch antenna and an observation point from the second patch antenna with respect to the origin. The α and β are the radial anticlockwise angles of the source and the observation point, respectively. The ε_0 is the relative dielectric constant of the free space and the f_r is the near resonance frequency of the disk patch antenna.

Now, consider Figure 3 where a satellite is flying around the Earth. The distance between the Earth and the satellite is changing in an orbit flight. Under the assumption that the satellite is approaching and moving away from the Earth, it is necessary to modify the EOC of the radiation pattern for providing a uniform power density on the Earth's surface. When the satellite is farthest, the field of view (FOV) is smallest and vice versa. Hence, as the required FOV is changing constantly in an orbit flight, the antenna array must reconfigure the radiation pattern in accordance to the altitude of the satellite and keep the uniform power density on the Earth's surface. Now, let us define a mask function $R_s(\theta, \varphi)$ as in [2] to know the FOV as well as the EOC in terms of the altitude of the satellite. The function $R_s(\theta, \varphi)$ indicates the relative distance of the antenna array mounted on a satellite to any point of the FOV and determines the angular position for the EOC.

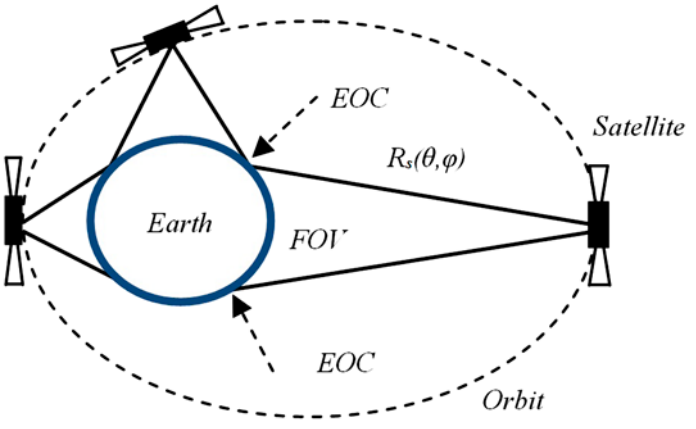

Figure 3. Flight of a satellite around the Earth at different altitudes.

The problem consists in finding the voltage excitations of the PAA in order to provide a reconfigurable pattern for different altitudes of the satellite. The reconfigurable pattern must be the best imitation of the shape of function $R_s(\theta, \varphi)$ and thereby, ensure a uniform power density on the Earth's surface. Otherwise, the side lobe level (SLL) of the reconfigurable pattern is required to be low. This aspect is recommended in order to generate less energy in the angular range that it is not illuminating the Earth. In addition, it could be noted that this lost energy might even interfere with other satellites or spacecrafts. At this point, let us define the next objective function:

$$of = P(\theta_{\mathrm{SLL}}, \varphi_{SLL}) + |P(\theta, \varphi) - R_s(\theta, \varphi)|^2 \quad (8)$$

where (θ_{SLL}, φ_{SLL}) is the angle direction where the maximum SLL is attained. The optimization is to minimize two aspects: firstly, the sum of the square error for each angle in the FOV zone between the shape of the Earth and the array factor; secondly, the maximum SLL. The fitness function was properly adjusted by weighting in each term with a trial and error method. The term of the error between the prescribed pattern and the isoflux radiation was weighted with a five coefficient and the term of the SLL was weighted with a unit coefficient.

2.1. Previous work

Different antenna array geometries for satellites applications instead of reflectors or horns has been designed.[18–20] These studies have focused mainly on multi-beam systems [21,22] and footprint radiations.[23,24] In addition, the isoflux radiation is very attractive for global broadcast services such as global positioning, weather forecast, television, and so on. Hence, different antenna array geometries have been designed for isoflux radiation.[2,13,14,25–28] These designs have been focused to generate a fixed isoflux pattern, i.e. the study has been focused onto satellites that do not change the altitude in an orbit flight such as geostationary Earth orbit (GEO) satellites, medium Earth orbit (MEO) satellites, and low Earth orbit (LEO) satellites. These previous designs have generated a fixed isoflux pattern by using linear, uniform quadrangular, aperiodic, concentric rings arrays, volumetric array, and anisotropic metasurface antenna.

Now, an interesting problem is to generate a reconfigurable isoflux pattern to ensure the power density on the Earth's surface for different altitudes of the satellite, i.e. for HEO satellites. The main contribution of this paper is the synthesis of reconfigurable isoflux radiation with the coupling effects of disk patches as elements of a concentric rings array. The elements of novelty, presented in this paper, are the application of evolutionary optimization techniques (PSO and HSA) to a design problem which is both nontrivial and interesting: the design of concentric rings antenna arrays for a reconfigurable isoflux pattern.

The next section presents the evolutionary optimization algorithms applied to this design problem.

3. The evolutionary optimization techniques

The objective of this paper is to design a concentric rings antenna array for a reconfigurable isoflux pattern. To deal with this problem, we propose to use HSA and PSO. We chose these algorithms for their ease of implementation and their efficiency for solving complex optimization problems.[29] Besides, their simplicity for implementation of the algorithms has shown to be of the most effective algorithms over an important set of difficult antenna design problems.[11,13] Notice that with this selection, we do not claim that HSA and PSO are the best options for this particular problem; determining the best optimization algorithm for a particular antenna design problem remains an open problem. Details of the procedure of each algorithm are given in the next section.

HSA algorithm is based on how the musicians of an orchestra play harmony. Each musician plays a different instrument with singular number of musical notes. Then, when the musicians improvise new notes with their own instruments, this generates a new harmony. If this new harmony is better, the new notes are adopted for the musician to the harmony. This procedure continues constantly by certain number of improvisations of each musician. When an optimal harmony is found, the algorithm converges. [10] The main steps of the implemented HSA are illustrated in detail in [11].

In the case of PSO, the particles within the swarm move influenced by its current position, its memory, and by the cooperation or social knowledge of the swarm,[9] using only one operator, the so-called velocity operator. Let us suppose a swarm of K particles, in which each particle $X_K = (x_{k1},\ldots, x_{kD})$ representing a potential solution is defined as a point in a D-dimensional space. The limits of the parameters x_{kd} to be optimized define the search space in D-dimensions. Iteratively, each particle k within the swarm flies over the solution space to a new position X_K with a velocity $V_K = (v_{k1},\ldots, v_{kD})$, both updated along each dimension d. The explanation of the steps for PSO has been widely explained in the previous works [13–14,26–27].

The parameters of HSA were tuned by a trial and error approach as follows: HMS = 200, NI = 6000, HMCR = 0.9, PAR = 0.3, $BW_I = 0.01$, and the initial CF = 2. The parameters of the implemented PSO are as follows: number of iterations NI = 500, number of particles $p_{\text{size}} = 200$, inertial weight w varies downward in the range of [0.95–0.4] through the optimization process, and the acceleration constants are $c_1 = c_2 = 2$. We follow the literature and our previous results to set the parameters of PSO [13–14,26–27]. Both the algorithms are configured with the same number of initial solutions, i.e. $HMS = p_{size}$. Those algorithms are performed to obtain the optimum excitations of the antenna elements with the above configurations. The results of optimization cases are detailed in the next section.

4. Simulation results

The HSA and PSO were performed by an Intel system i7-860 with 8 Gb of memory RAM. The array consists of $N_T = 61$ antenna elements distributed in $N_r = 4$ rings plus a central element. The rings contain 6, 12, 18, and 24 antenna elements, respectively. The near resonant frequency of the disk patch antennas is 8.2 GHz. The radio of the patch is $a = 2.0862$ cm according to [21]. The substrate thickness is $h = 0.1071$ cm with a relative dielectric constant of $e_r = 2.1$. The maximum aperture of the PAA is of 59.8645 cm for the specified frequency. The feeder of each patch is positioned at 5.7315 mm distance from the center in order to match the antennas to a coaxial cable of 50Ω of impedance. This design permits to obtain different patterns by only obtaining the required excitation coefficients, i.e. it is possible to configure the array for any EOC. Let us show three examples of the pattern reconfigurability when the satellite is flying at 36000, 20000, and 2000 km. These altitudes must be configured for an isoflux curvature of 18°, 28° and 100°, respectively.[2] In this case, the mask $R_s(\theta, \varphi)$ is a priori configured for those specific considerations. The HSA and PSO obtained the optimal excitations for each patterns. Both algorithms were performed by optimizing the optimum vector of current excitations I and then by the calculation of the impedance matrix Z; the optimum values of the voltage excitations L are obtained.

Figures 4–6 show the normalized radiation pattern $P(\theta, \varphi)$ for each reconfigurable pattern example. These figures show also the results obtained by the HSA and the PSO. Both algorithms found out very similar radiation patterns. For the case of 18° and 28°

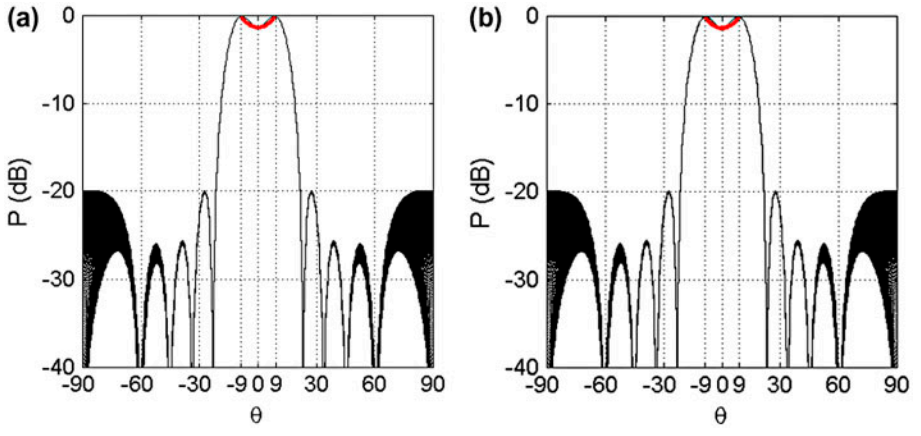

Figure 4. Reconfigurable Pattern $P(\theta,\varphi)$ for 36,000 km of altitude: (a) HSA and (b) PSO.

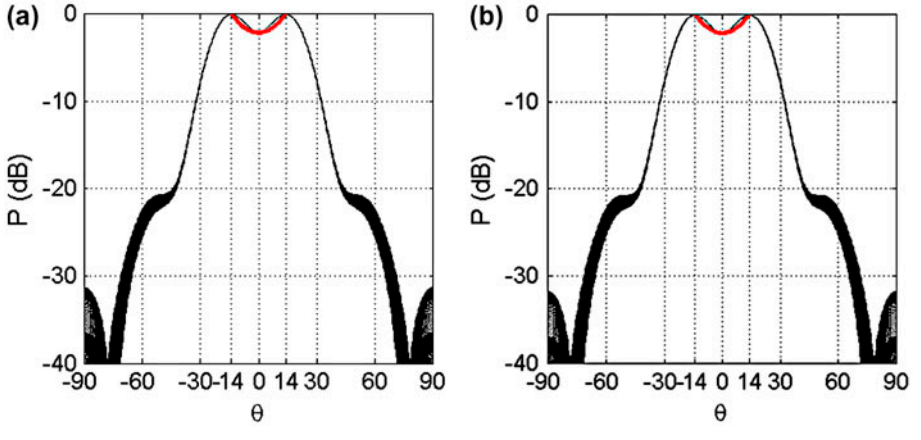

Figure 5. Reconfigurable Pattern $P(\theta,\varphi)$ for 20,000 km of altitude: (a) HSA and (b) PSO.

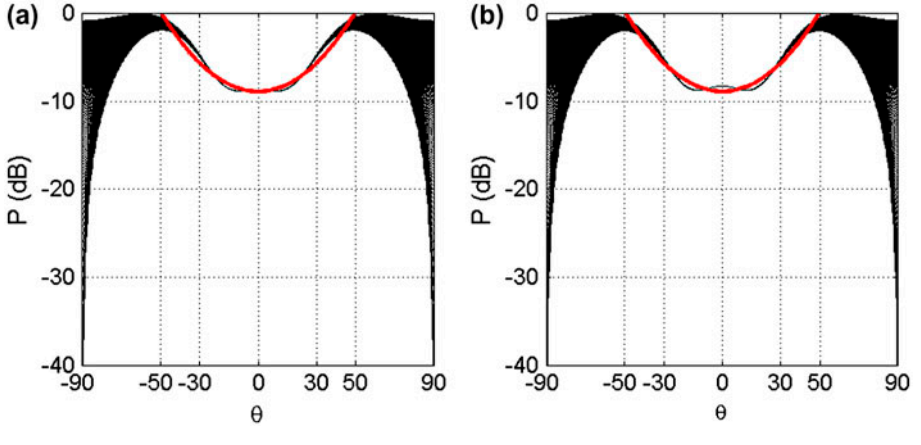

Figure 6. Reconfigurable Pattern $P(\theta,\varphi)$ for 2000 km of altitude: (a) HSA and (b) PSO.

degrees of isoflux curvature (see Figures 4 and 5), the mask and the radiation pattern illustrate a good accuracy with a SLL reduction of < -20 dB. In the case of coverage of 100° (see Figure 6), there is an effect of the disk patch antennas that generate a deviation in the maximum of the pattern (at the edge of view, for around 2 dB with respect to the cut of $\varphi = 0°$ and $\varphi = 90°$). Since the point of view that the Earth is not a perfect sphere exists, this fact does not affect substantially the performance of the radiation. Moreover, this particular pattern does not have any side lobe due to the wide coverage in the elevation plane. Anyway, for the three cases, the pattern permits an acceptable accuracy in a wide coverage whereas the maximum radiation was obtained in the EOC.

Figures 7 and 8 show the antenna excitations distributions for each disk patch antenna marked by certain color. Figure 7 shows the levels of current excitations; the reconfigurability of the array is accomplished by turning off and turning on the antenna elements of each ring. In this case, three levels of current excitations are always kept

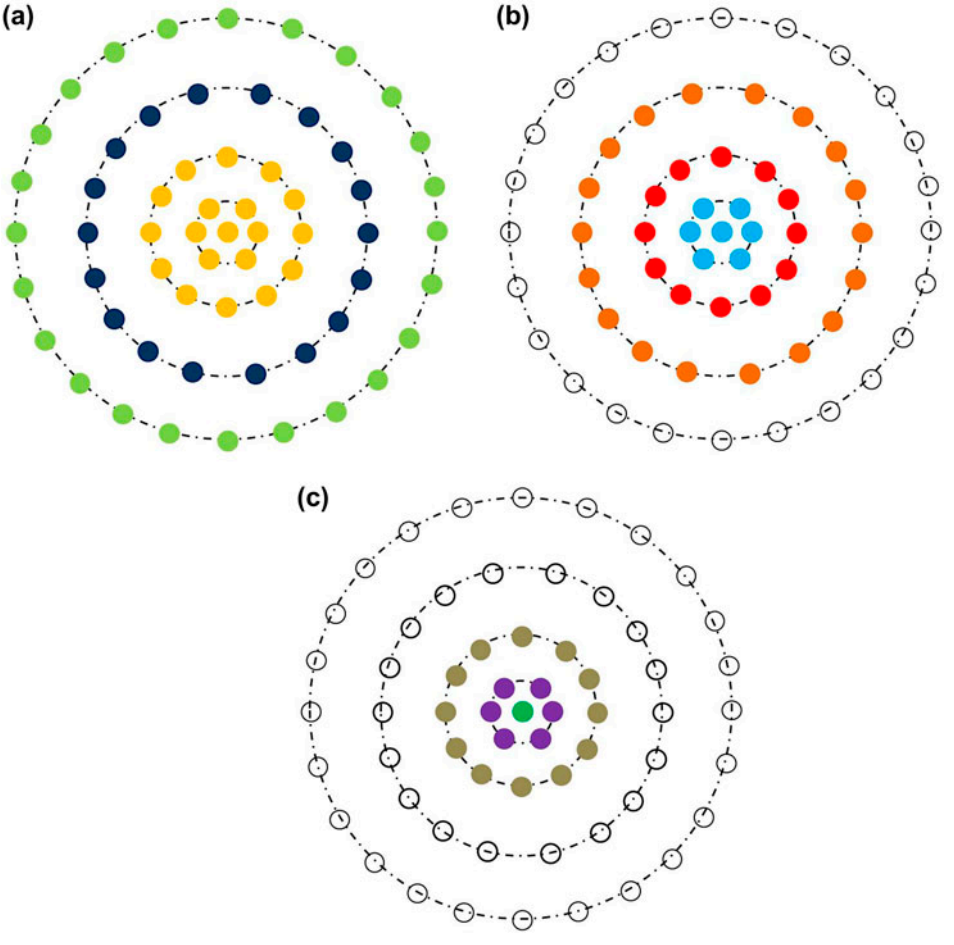

Figure 7. Current excitation distribution (I) for patterns of different coverage: (a) 18°,(a) 28°, and (a) 100°.

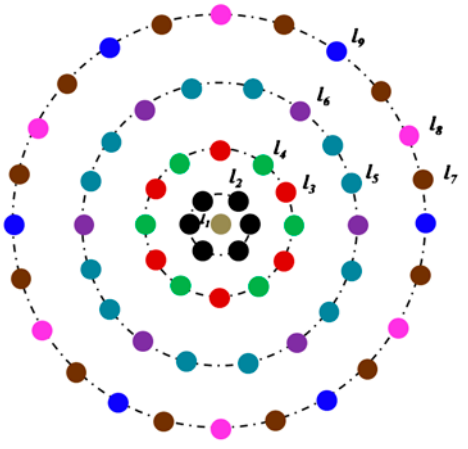

Figure 8. Voltage excitation distribution (L) for the three cases of coverage.

for each case of pattern. In order to compensate the coupling effects, the voltage excitations L are obtained by solving the impedance matrix Z (see Equation 3).

Figure 8 illustrates that every antenna element of the rings 2, 3, and 4 have a different perspective of visibility with respect to the antenna elements of first ring and the center element. This fact alters the mutual impedances. Furthermore, note that the rings 2, 3, and 4 have 2, 2, and 3 levels of voltages, respectively. That is because of the effect of mutual coupling included in the mutual impedances within the impedance matrix. The levels of voltage excitations are slightly different due to the mutual impedances among the patches.[12,17] In this case, the antenna array consists in nine voltage excitations which permit three current excitations for the different radiation patterns. As an important aspect, the disk patch permits the use of a few levels of excitations due to the similar perspectives of visibility that the patch has within the array. This cannot be achieved by a square patch antenna which requires a major amount of levels of voltage excitation to compensate the mutual coupling effects. A PAA with square patches need more levels of voltage excitations for keeping the same current excitations. Hence, it is preferable, the use of disk patch antennas for reducing the size, weight, and complexity of the feeding network and heat dissipation systems.

Finally, Table 1 presents the numerical data of the optimization. The values of the voltage and current excitations are included in this Table. Only nine levels of voltages excitations and three levels of current excitations are observed; undoubtedly, since it is not necessary to control a great amount of antenna excitations to provide the reconfigurability, this reduces the complexity of the feeding and heat dissipations systems. Hence, we can affirm that the use of an optimum PAA could be suitable to reduce the mass and weight of the whole antenna array for this application. Moreover, note in the table that although the HSA was run for more number of iterations, it lasted around 10 min of optimization time to obtain the current excitations. In this case, the PSO lasted around 170 min of optimization time to obtain the current excitations since it was configured for a major number of evaluations. The column 7 shows the time where optimization reached the optimum solution, i.e. the time where the algorithms started to converge.

Table 1. Numerical values for the optimization cases.

Algorithm	Coverage	L (voltage excitations)	I (Current excitations)	SLL (dB)	Optimization time (minutes)	Time for convergence (minutes)
HSA	18°	3.9272 + 9.8793i 65.7937 + 46.2149i 45.3106 + 12.1722i 43.5863 + 10.1878i, 18.5724 + 4.0618i, 19.0009 + 4.1585i, −10.3793 − 0.1496i, −10.1864 + 0.0204i, −10.9593 + 0.1913i	0.6847, 0.1325, −0.2218,	−19.8947	10.0549	3.0365
	28°	13.8589 + 33.4766i 23.1353 + 12.0200i 2.8450 + 2.5933i 2.0827 + 1.7185i, − 3.4978 − 1.0427i, − 3.2565 − 0.7352i, −0.4408 + 0.1419i, −0.2807 + 0.0711i, −0.6151 + 0.2315i	0.3027, 0.0250, −0.0446	−31.2819	10.8274	2.5841
	100°	43.0410 − 4.9744i, −7.6834 +11.6589i, −5.0930 − 6.4223i, −4.7495 − 6.0276i, 5.2096 − 1.9372i, 5.0960 − 2.1007i, 2.3458 + 2.9918i, 2.2657 + 3.0251i, 2.4178 + 2.9693i	0.8621, −0.1364, 0.0146	Not applied	10.6651	9.3355

(*Continued*)

Table 1. (*Continued*).

Algorithm	Coverage	L (voltage excitations)	I (Current excitations)	SLL (dB)	Optimization time (minutes)	Time for convergence (minutes)
PSO	18°	−4.4031 − 11.0428i, −74.0062 − 52.0004i, −50.9579 − 13.6677i, −49.0185 − 11.4358i, −20.9124 − 4.5942i, −21.3943 − 4.7030i, 11.7345 + 0.1893i, 11.5175 − 0.0020i, 12.3869 − 0.1939i	−0.7701, −0.1494, 0.2504	−19.8849	169.4626	86.4259
	28°	42.8254 + 104.4130i, 72.4290 + 37.5708i, 8.9862 + 8.2112i, 6.6051 + 5.4788i, −11.0763 − 3.3959i, −10.3231 − 2.4387i, −1.3504 + 0.5121i, −0.8513 + 0.2907i, −1.8956 + 0.7945i	0.9455, 0.0815, −0.1427	−31.7509	175.1633	105.0979
	100°	36.5611 − 4.5705i, −6.6377 + 9.9287i, −4.2615 − 5.4563i, −3.9638 − 5.1143i, 4.4910 − 1.6717i, 4.3922 − 1.8150i, 2.0220 + 2.5766i, 1.9521 + 2.6061i, 2.0839 + 2.5577i	0.7348, −0.1182, 0.01434	Not applied	168.3938	60.6217

5. Conclusions

The authors proposed a novel design of a PAA for a reconfigurable isoflux pattern. The geometry of concentric ring array with disk patch antennas could provide a solution for reducing the volume occupation and complex feeding and heat dissipation systems in a satellite antenna system. The design considers only nine levels of voltage excitations. That permits three levels of current excitations with 61 antenna elements. In fact, this design could be applied to other types of patterns that require limited number of antenna elements and excitations. Besides, the novelty of this study also relies on the application of PSO and HSA in order to optimize PAA for the problem related to the synthesis of a reconfigurable pattern with simplification of the hardware.

Acknowledgments

This work was supported by the Mexican National Science and Technology Council under the grant 127919.

References

[1] Ippolito LJ, Jr. Satellite communications systems engineering: atmospheric effects, satellite link design and system performance. Washington (DC): Wiley; 2008.
[2] Vigano MC, Toso G, Angeletti P, Lager IE, Yarovoy A, Caratelli D. Sparse antenna array for Earth coverage satellite applications. Proceedings of the Fourth European Conference on Antennas and Propagation; 2010 April; Barcelona. (ES).
[3] Rainer S, Roeser H-P, Valenzuela A. Small satellite missions for Earth observation: new developments and trends. Heidelberg: Springer; 2010.
[4] Brown DL. HEO spacecraft and lunch scenarios. IEE colloquium on Highly Elliptical Orbit Satellite Systems; 1989 may.
[5] Yates L. HEO or GEO? Commun. Eng. 2007;5:40–45.
[6] Garg R. Microstrip antenna design handbook. Norwood (OH): Artech House; 2001.
[7] Lee KF, Luk KM. Microstrip patch antennas. London: Imperial College Press; 2011.
[8] Hon Tat Hui. Decoupling methods for the mutual coupling effects in antenna arrays: a review. Rece. Pat. Eng. 2007;1:187–193.
[9] Eberhart RC, Shi Y. Particle swarm optimization: developments, applications and resources. In: Proceedings Congress, Evolutionary Computation; 2001, 81–86.
[10] Geem ZW, Kim JH, Loganathan GV. A new heuristic optimization algorithm: harmony search. Simulation. 2001;76:60–68.
[11] Guney K, Onay M. Optimal synthesis of linear antenna arrays using a harmony search algorithm. Expert Syst. Appl. 2011;38:15455–15462.
[12] Balanis C. Antenna theory: analysis and design. 2nd ed. New York (NY): Wiley; 1997.
[13] Reyna Alberto, Panduro Marco A, Del Rio Carlos. Design of concentric ring antenna arrays for isoflux radiation in GEO satellites. IEICE Electron. Express. 2011;8:484–490.
[14] Reyna A, Panduro MA, del Rio-Bocio C. On the design of concentric ring arrays for isoflux radiation in MEO satellites based on PSO. Prog. Elect. Res. M. 2011;20:243–255.
[15] Schellkunoff SA. Some equivalence theorems of electromagnetics and their application to radiation problems. Bell Sys. Tech. 1936;15:92–112.
[16] Volakis JL. Antenna engineering handbook. 4th ed. New York (NY): McGraw Hill; 2007.
[17] Bhattacharjee Partha S. Mutual impedance between circular microstrip antenna. Micro. Opt. Tech. Lett. 1993;6:322–325.
[18] Kyung-Jin Jeon, Kyo-il Lee, Jae-gi Son; Taek-Kyung Lee, Lee J-W, Woo-Kyung Lee. X-band isoflux pattern antenna for SAR data transmission. Synthetic Aperture Radar (APSAR), 2011 3rd International Asia-Pacific Conference on; 2011 September.
[19] del Rio, Fernandez JE, Nubla A, Bustamante L, Vila F, Klooster K, van't, Frandsen A. Novel isoflux antenna alternative for LEO satellites downlink. 29th European Microwave Conference; 1999 October.

[20] Jan Zackrisson, J. Bäck. Wide coverage antennas. TTC 2004 Workshop, ESA WPP-230; 2004 September.
[21] Kenneth N. Sherman. Phased array shaped multi-beam optimization for LEO satellite communications using a genetic algorithm. Proceedings 2000 IEEE International Conference on Phased Array Systems and Technology; 2002.
[22] Vigano MC, Toso G, Caille G, Mangenot C, Lager IE. Sunflower array antenna with adjustable density taper. Int. J. Antennas Propag. 2009; 2009:1–11.
[23] Ares F, Fondevila-Gomez J, Franceschetti G, Moreno-Piquero E, Rodriguez-Gonzalez JA. Synthesis of very large planar arrays for prescribed footprint illumination. IEEE Trans. Antennas Propag. 2008;56:584–589.
[24] Villegas FJ. Parallel genetic-algorithm optimization of shaped beam coverage areas using planar 2-D phased arrays. IEEE Trans. Antennas Propag. 2007;55:1745–1753.
[25] Morabito AF, Lagana AR, Isernia T. On the optimal synthesis of ring symmetric shaped patterns by means of uniformly spaced planar arrays. Prog. Elect. Res. B. 2010;20:33–48.
[26] Reyna Alberto, Panduro Marco A, del Rio-Bocio Carlos. Design of aperiodic planar arrays for isoflux radiation in GEO satellites by applying evolutionary optimization. Expert Syst. Appl. 2012;39:6872–6878.
[27] Alberto Reyna, Marco A. Panduro, Carlos del Rio-Bocio. Volumetric ring array for uniform global coverage in satellite applications. Proceedings of International Symposium on Antennas and Propagation; 2012 July, Chicago IL (USA).
[28] Minatti G, Maci S De, Vita P, Freni A, Sabbadini M. A circularly-polarized isoflux antenna based on anisotropic metasurface. IEEE Trans. Antennas Propag. 2012;60:4998–5009.
[29] Lee Kang Seok, Geem Zong Woo. A new meta-heuristic algorithm for continuous engineering optimization: harmony search theory and practice. Comput. Method. Appl. M. 2005;194:3902–3933.